High localization, focal depth and contrast by means of nonlinear Bessel Beams

Paolo Polesana, Daniele Faccio, Paolo Di Trapani

Universitá degli Studi dell'Insubria, Via Valleggio 2 Como (Italy)

paolo.polesana@uninsubria.it daniele.faccio@uninsubria.it paolo.ditrapani@uninsubria.it

Audrius Dubietis, Algis Piskarskas

Department of Quantum Electronics, Vilnius University, Sauletekio ave. 9, bldg. 3, LT-10222 Vilnius, Lithuania

audrius.dubietis@ff.vu.lt; algis.piskarskas@ff.vu.lt

Arnaud Couairon

Centre de Physique Theorique CNRS UMR 7644, Ecole Polytechnique, F-91128 Palaiseau Cedex, FRANCE

couairon@cpht.polytechnique.fr

Miguel A. Porras

Departamento de Fisica Aplicada, ETSIM, Universitad Politécnica de Madrid, Rios Rosas 21, 28003 Madrid, Spain

porras@dfarn.upm.es

Abstract: We show an experimental and computational comparison between the resolution power, the contrast and the focal depth of a nonlinearly propagated diffraction-free beam and of other beams (a linear and a nonlinearly propagated Gaussian pulse): launching a nondiffractive Bessel pulse in a solution of Coumarine 120 in methanol creates a high contrast, 40 mm long, 10 μm width fluorescence channel excited by 3-photon absorption process. This fluorescence channel exhibits the same contrast and resolution of a tightly focused Gaussian pulse, but reaches a focal depth that outclasses by orders of magnitude that reached by an equivalent Gaussian pulse.

OCIS codes: (190.4180) Multiphoton processes; (190.5530) Pulse propagation and solitons

References and links

1. J. Durnin, J.J. Micheli and J.H. Heberly: "Diffraction-Free Beams," Phys. Rev. Lett. **58**, 1499-1501 (1987)
2. H. Sõnajalg, M. Rätsep and P. Saari: "Demonstration of the Bessel-X pulse propagating with strong lateral and longitudinal localization in dispersive medium," Opt. Lett. **22**, 310-312 (1996)
3. D. McGloin and K. Dholakia: "Bessel beams: diffraction in a new light," Contemporary Physics **46**, 15-28 (2005)
4. S. Orlov, A. Piskarskas and A. Stabinis: "Localized optical subcycle pulses in dispersive media," Opt. Lett. **27**, 2167-2169 (2002)
5. R. Grunwald, V. Kebbel, U. Griebner, U. Neumann, A. Kummrow, M. Rini, E. T. J. Nibbering, M. Piche, G. Rousseau and M. Fortin: "Generation and characterization of spatially and temporally localized few-cycle optical wave packets," Phys. Rev. A **67**, 063820 (2003).
6. T. Wulle, S. Herminghaus: "Nonlinear Optics of Bessel Beams," Phys. Rev. Lett. **70**, 1401-1403 (1993)

#8057 - $15.00 US Received 8 July 2005; revised 27 July 2005; accepted 29 July 2005

7. R. Gadonas, A. Marcinkevicius, A. Piskarskas, V. Smilgevicius, A. Stabinis: "Traveling wave optical parametric generator pumped by a conical beam," Opt. Commun. **146**, 253-256 (1998)
8. M.A. Porras, A. Parola, D. Faccio, A. Dubietis and P. Di Trapani: "Nonlinear Unbalanced Bessel beams: stationary conical waves supported by nonlinear losses," Phys. Rev. Lett. **93**, 153902 (2004)
9. H. Schroeder, S.L. Chin: "Visualization of the evolution of multiple filaments in methanol," Opt. Commun. **234** 399-406 (2004)
10. T. Brabec, F. Krausz: "Nonlinear Optical Pulse Propagation in the Single-Cycle Regime," Phys. Rev. Lett. **78**, 3282-3285 (1997)
11. A. M. Perelomov, V. S. Popov and M. V. Terent'ev: "Ionization of atoms in an alternating electric field," Sov. Phys. JETP **23**, 924-934 (1966)
12. A. Dubietis, E. Gaižauskas, G. Tamošauskas and P. Di Trapani: "Light filaments without self channeling," Phys. Rev. Lett. **92**, 253903 (2004)
13. W. Liu, S.L. Chin, O. Kosareva, I.S. Golubtsov, V.P. Kandidov: "Multiple refocusing of a femtosecond laser pulse in a dispersive liquid (methanol)," Opt. Commun. **225**, 193-209 (2003)
14. M. Erdelyi, Z. L. Horvath, G.Szabo, Zs. Bor, F.K. Tittel, J.R. Cavallaro and M.C. Smayling: "Generation of diffraction-free beams for applications in optical microlithography," J. Vac. Sci. Technol. **B** 15, 287-292 (1997)
15. J. Amako, D. Sawaki and E. Fujii: "Microstructuring transparent materials by use of nondiffracting ultrashort pulse beams generated by diffractive optics," J. Opt. Soc. Am. B **20**, 2562-2568 (2003)

1. Introduction

Conical waves are unique and peculiar wave packets, in which the energy flow is not directed along the beam axis, as in conventional waves. In contrast, here the energy arrives laterally, i.e., from a cone-shaped surface, leading to the appearance of a very intense and localized interference peak at the cone vertex. Significant examples of conical waves are Bessel (or Durnin) beams [1] in the continuous-wave limit, and "X waves", in the ultra-short pulse regime which exhibit stationarity also in presence of material chromatic dispersion [2]. To date, conical wave packets (CWP) have mostly been considered for applications in the linear regime (see review in ref. [3]).

In the linear case the key feature addressed in the literature is the property of exhibiting a very localized peak, both in transverse (down to a few wavelengths) and longitudinal (down to a few cycles) coordinates [4, 5]. This peak propagates free of diffraction and dispersion, even in dispersive materials, over distances that outclass by orders of magnitudes those achievable with conventional Gaussian-like beams. The drawback is that such a peak is supported by the presence of slowly decaying tails, which contain the larger part of the wave energy. These tails extend far from the peak. Consequently, the overall wave packet does not behave as a genuine localized wave, but rather as an extended wave. Thus, for example, if a Bessel beam is used for linear microscopy, owing to its non-diffractive property, very small objects deep inside a thick transparent sample can indeed be detected; this is not possible with Gaussian-like beams. However, due to the presence of large side lobes, both the contrast and the quality of the final image are reduced dramatically, which renders the option unsuitable for breakthrough in applications. This explains why conical waves have not made a breakthrough in field applications, until now.

This article aims to demonstrate the novel approach of exploitation of conical waves in the non-linear regime, i.e., in conditions where the material responds only to the high-intensity (or hot) part of the wave, and is transparent to the weak (or cold) portion. Previous works about nonlinear properties of conical waves concern for example SHG [6] and parametric processes [7]: in these fields the vectorial (e.g. phase-matching) properties of the conical wave were investigated. Our approach, instead, is centered on the characteristics of the spatial profile of the nonlinear polarization arising from multi-photon interactions. In these operating conditions, never considered before, the cold part of the wave will behave as a reservoir traveling locked to the hot peak. This cold reservoir stores a major amount of energy and continually refills the hot peak where energy exchange with matter and/or dissipation typically take place due to the nonlinear matter response (see ref. [8]). In this case the unique non-diffractive and non-dispersive

#8057 - $15.00 US Received 8 July 2005; revised 27 July 2005; accepted 29 July 2005

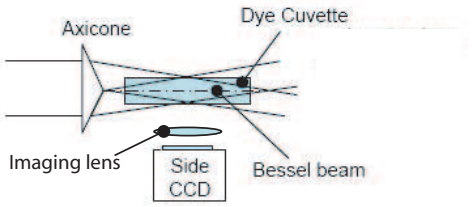

Fig. 1. Experimental setup. A linearly polarized Gaussian 1055 nm wavelength, 1 ps pulse is converted into a Bessel pulse using an axicon with 2.3 degrees base angle. The Bessel pulse (which remains focused on a 10 cm distance) passes through a 4 cm cell filled with a light Coumarine 120 methanol solution. 3-photon fluorescence is recorded by CCD side imaging.

properties of conical waves will reveal a dramatic potential for applications. In fact, the peculiar properties of nonlinear conical waves ensure stationarity and maintenance of a high degree of localization of the interaction region (the hot spot) over a very long path inside the material, which is not possible either for Gaussian or for linear conical waves.

Nonlinear energy dissipation accompanies collapse of wave-packets in virtually all physical systems. The stationarity of CWP's in the presence of non-linear losses claimed above therefore suggests that a crucial role is played by CWP's in the case of collapse or in strong-localization processes. This simple but original claim, which connects the non-linear losses with the "geometry" of the process, opens up a new perspective in non-linear wave physics.

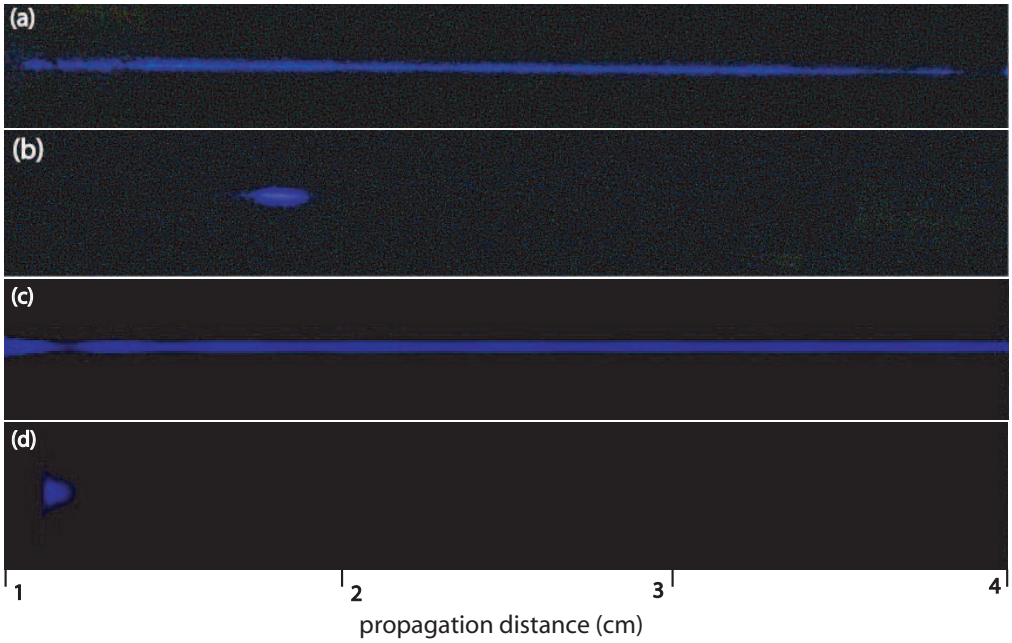

Fig. 2. (a): Fluorescence channel generated by a Bessel beam; total energy: 1000 μJ; central-peak energy: 15 μJ; beam length: 1 ps; Bessel's FWHM: 20 μm; axicon illuminated by a 4 mm FWHM Gaussian beam. (b): Fluorescence channel generated by a pulsed Gaussian beam of the same FWHM diameter; input energy: 70 μJ; (c-d): Numerical results relative to the two cases of above (see text for details)

#8057 - $15.00 US
Received 8 July 2005; revised 27 July 2005; accepted 29 July 2005

2. Nonlinear loss localization: experimental evidence

In a first experiment we filled a 4 cm long cuvette with a solution of methanol and Coumarine 120. The fluorescence channel is excited by launching a 1 ps, 1 mJ, 1055 nm linearly polarized pulsed Bessel beam, generated by transmitting a 4mm FWHM Gaussian beam through an axicon with 2.3 degrees base angle. With this setting, the Gaussian-apodized Bessel beam creates a 20μm FWHM central spike (as also experimentally verified), whose energy (within the first-zero circle) is of 15 μJ. A schematic description of the experimental apparatus is presented in Fig. 1.

Figure 2(a) reports the result of the measurement of the fluorescence-channel profile, excited in the Coumarine solution *via* three-photon absorption (TPA) (the Coumarone absorption peak is located at 350 nm). The detection has been performed by side imaging *via* a commercial CCD photo camera (Canon-EOS D30). Fig. 2(b) illustrates for comparison the fluorescence channel generated when a 1 ps, 70 μJ, 1055 nm, 20μm FWHM pulsed Gaussian beam was launched with the beam waist located inside the cuvette. As expected, a high contrast, high focal depth, ultra thin fluorescence channel is excited in the case of Bessel-beam illumination.

In a second experiment we launched in the Coumarine 120 solution a continuous wave (CW) 532 nm Bessel beam, generated by transmitting a 4 mm FWHM Gaussian beam through the same axicon (source was a 10 mW solid state laser). With this setting, the Gaussian-apodized Bessel beam is expected to create a 10 μm FWHM central spike. Owing to the very low power, only linear interaction (*e.g.* one-photon scattering process) is expected to occur.

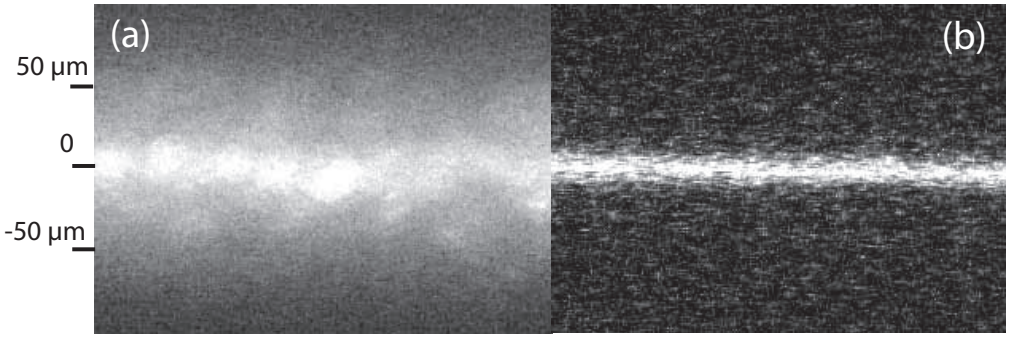

Fig. 3. (a): Comparison between linear scattering of a linear Bessel beam (527 nm wavelength and 10 μm FWHM) and (b) the trace left by the 3-photon fluorescence lit by a Bessel pulse of 20 μm of FWHM when intensity is high (1 mJ at 1 ps with 1055 nm wavelength).

Figure 3(a) reports the measurement of the scattered light, acquired with the identical detection apparatus as in Fig. 2(a) and 2(b). Note how, in spite of the twice smaller central spike, the scattering process in linear regime fills a much broader area, owing to the contribution of Bessel's side lobes to the scattering process. This result unambiguously demonstrates the advantage of exciting the channel in multi-photon absorption regime. We mention that direct measurement of the linear scattering generated by the 1055 nm pulsed Bessel beam was prevented owing to cut off in sensitivity of our CCD in the infrared spectral region. Figure 3(b) reports a zoomed portion of Fig. 2(a) for comparison.

3. Nonlinear loss localization: model and simulations

A better comprehension of the phenomenon can be achieved by means of numeric simulations. We performed a calculation of the propagation of Gaussian apodized pulsed Bessel beams (wavelength 1055 nm, pulse duration 1 ps, FWHM 20 μm ,energy 1 mJ) and of pulsed Gaussian

#8057 - $15.00 US Received 8 July 2005; revised 27 July 2005; accepted 29 July 2005

beam (wavelength 1055 nm, pulse duration 1 ps, FWHM 20 μm , energy 15 μJ) in a Coumarine 120 methanol solution. The energy and the dimensions of the Gaussian beam have been chosen to fit the characteristics of the Bessel beam's central spot. Note that if we focus the entire 1 mJ energy in the same 20 μm diameter we induce material breakdown. Moreover, the same amount of energy focused in much broader areas leads to multiple filamentation [9]: both of these regimes are unsuitable for the applications here suggested.

The nonlinear properties of the medium are Kerr self focusing (with a coefficient for nonlinear refraction index n_2 = 4.7000e-16 cm^2/W) and 3-photon absorption. The propagation equation solved by the code is an extended nonlinear Schrödinger equation [10]: it describes the propagation along the z axis of the envelope of the laser field with central frequency ω_0:

$$\hat{U}\frac{\partial\hat{\mathscr{E}}}{\partial z} = i[\frac{\nabla_\perp^2}{2k} + \frac{k}{2}\left(\frac{n^2\omega^2}{k^2c^2} - \hat{U}^2\right)]\hat{\mathscr{E}} + \mathrm{TF}\{N(\mathscr{E})\}, \tag{1}$$

where $\hat{\mathscr{E}}(r,\omega,z) = \mathrm{TF}\{\mathscr{E}(r,t,z)\}$ (TF stands for time Fourier transform), $\hat{U}(\omega) \equiv 1 + (\omega - \omega_0)/kv_g$, $v_g \equiv \partial\omega/\partial k|_{\omega_0}$ is the group velocity and $\mathrm{TF}\{N(\mathscr{E})\}$ the time-Fourier transform of the nonlinear terms. Here $n(\omega)$ denotes the linear refraction index. The nonlinear terms is

$$N(\mathscr{E}) = SF[\mathscr{E}(t)] + NLL[\mathscr{E}(t)] \tag{2}$$

$$SF[\mathscr{E}(t)] = ik_0n_2T^2|\mathscr{E}(t)|^2\mathscr{E}(t) \tag{3}$$

$$NLL[\mathscr{E}(t)] = -T\frac{\beta_K}{2}\rho|\mathscr{E}|^{2K-2}\mathscr{E} \tag{4}$$

The operator $T \equiv 1 + \frac{i}{\omega_0}\frac{\partial}{\partial t}$ accounts for pulse self-steepening; ρ is the molar concentration of the multiphoton absorber (10% in this case). Factor β_K (K = 3) is computed with Keldysh formula [11] ($\beta_3 = 2.220710^{-22}$ cm^5/J^2). Bessel beam is apodized with a Gaussian mask with a FWHM of 4 mm, so that the input pulse in the simulation is not an idealized radially infinite one, but a real world pulsed Bessel beam.

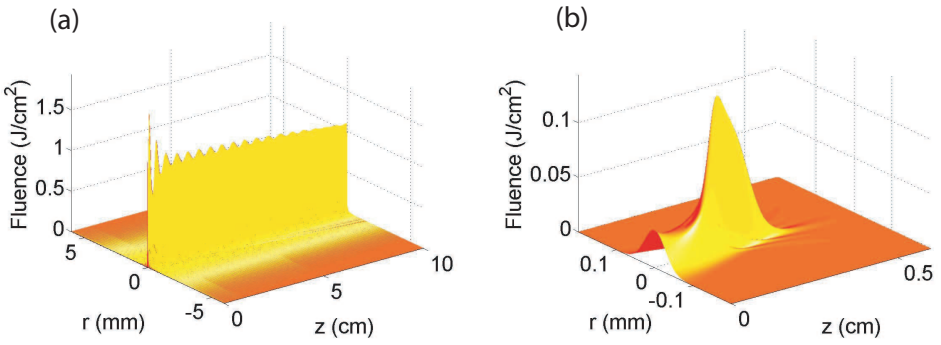

Fig. 4. (a): fluence profile of a pulsed Bessel beam (1 ps, 20 μm FWHM, 1 mJ 1055nm wavelength pulse) launched in a Coumarine 120 methanol 10% molar solution. The dye has an absorption peak at 350 nm corresponding to a 3-photon absorption. (b): a great difference in behavior is observed for a Gaussian beam of the same FWHM diameter with energy equal to the energy contained within the first zero of the Bessel beam (15 μJ). Note the different z scale with respect to (a)

A study of the localization of nonlinear losses has been carried out by considering the term $NLL[\mathscr{E}(t)]$ in Eq. (4) and the intensity profiles obtained by integration of the propagation equa-

#8057 - $15.00 US
Received 8 July 2005; revised 27 July 2005; accepted 29 July 2005

tion Eq. (1). We perform for this analysis a small $\omega - \omega_0$ expansion for the linear refraction index $n(\omega)$ and neglect the departure from unity in the operators $\hat{U}$ in Eq. (1) and T in Eq. (3) and (4) (which is a good approximation for our long pulses). We obtain the evolution equation for the intensity:

$$\frac{\partial I(r,z,t)}{\partial z} = \mathscr{D}(r,z,t) - \mathscr{L}(r,z,t) \tag{5}$$

$$\text{with } \mathscr{D}(r,z,t) = (i/2k)(\mathscr{E}^*\Delta_\perp^2\mathscr{E} - \mathscr{E}\Delta_\perp^2\mathscr{E}^*) - ik''(\mathscr{E}^*\frac{\partial^2\mathscr{E}}{\partial t^2} - \mathscr{E}\frac{\partial^2\mathscr{E}^*}{\partial t^2}) \tag{6}$$

$$\text{and } \mathscr{L}(r,z,t) = \beta_K \rho I^K(r,z,t) \tag{7}$$

where $k'' = \partial^2 k/\partial\omega^2$ and I is the intensity ($I \propto \mathscr{E}\cdot\mathscr{E}^*$).

The term $\mathscr{D}$ accounts for the intensity redistribution due to diffraction and dispersion while $\mathscr{L}$ is the density of three photon absorption. Once calculated the intensity profile $I(r,z,t)$ from Eq. (1), we integrate in time this density:

$$L(z,r) = \int_t \mathscr{L}(r,z,t)dt \tag{8}$$

that represents the energy density loss due to nonlinear absorption (measured in J/cm ^{3}). Since the only absorption mechanism is three photon absorption, we expect the fluorescence to be proportional to $L(z,r)$.

4. Simulation results

The results of the propagation of the two pulses are reported in Fig. 4. Here, the fluence profile defined as $F(r,z) = \int dt I(r,t,z)$ is plotted as a function of the radial coordinate and the propagation distance for the nonlinear Bessel (Fig. 4(a)) and the Gaussian (Fig. 4(b)) pulses. Figure 5 shows energy losses due to three photon absorption (function $L(r,z)$ defined by Eq. (8)) in J/cm^3 as a function of the propagation distance and radius both for the Bessel (Fig. 5(a)) and the Gaussian (Fig. 5(b)) pulse. Figure 6 shows the beam width at half maximum as a function of the propagation distance of the Bessel (Fig. 6(a)) and the Gaussian (Fig. 6(b)) pulses. For comparison, the beam width obtained by linear propagation of the same pulses is plotted in dashed curves.

Figure 2(c) and 2(d) show the energy density losses (Eq. 8) as a function of the propagation distance. The integration mimics the actual measurement procedure, which accumulates fluorescence light generated by all transverse planes at different depth in the sample.

5. Discussion of the results

Propagation, simulated over 10 cm show that the Bessel central peak after a few strong oscillations arrives to a stationary radial profile maintained over the whole propagation length as shown in Fig. 4(a). On the contrary nonlinear propagation of the Gaussian beam (Fig. 4(b)) is characterized by the complete dissipation of the pulse, which exhausts after a few millimeters without having reached any stationary profile and reaches a fluence peak much lower than in the case of the pulsed Bessel beam (about 1.5 J/cm^2 for the Bessel pulse, just 0.1 J/cm^2 for the Gaussian). The robustness of the conical wave against strongly nonlinear propagation is due to the fact that nonlinear losses are compensated thanks to the continuous refilling of the hot core by linearly propagated energy coming from the outer rings. Figure 5(a), which plots function $L(r,z,t)$ computed on the Bessel beam, clearly shows that absorption involves just the central peak, while outer rings propagate quite untouched. So although 42.5% of the total energy is absorbed in 10 cm, the central peak profile remains unchanged. This is not true for the

#8057 - $15.00 US Received 8 July 2005; revised 27 July 2005; accepted 29 July 2005

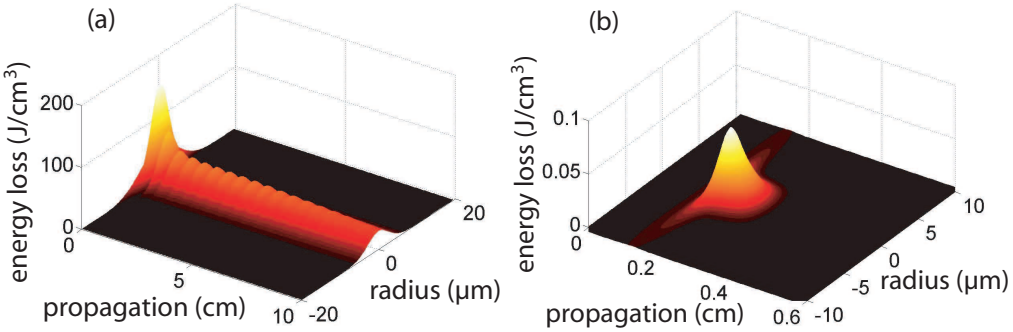

Fig. 5. (a) Energy nonlinear loss profile (function $L(r,z)$) computed on the Bessel (1 ps, 20 μm FWHM, 1 mJ 1055nm wavelength pulse) propagation. Comparison is made with the same computation on the propagation of a Gaussian beam (1 ps, 20 μm FWHM, 15 μJ 1055nm wavelength pulse) (b) of the same energy and FWHM as Bessel's pulse central spot.

Gaussian beam, whose energy dissipation process shown in Fig. 5(b) involves all the beam. For this reason dissipation reaches 82.5% and completely destroys the beam in just 4 mm (a crude estimation of the loss can be argued from Fig 5b: $\pi \cdot (3\mu\text{m})^2 \cdot 0.1\text{cm} \cdot 0.1\text{J/cm}^3 = 10\mu\text{J}$ corresponding to 66% energy loss). Moreover, the fact that nonlinear absorption involves just the central peak of the Bessel pulse, implies a great enhancement in contrast for the generated fluorescence with respect to the linear slow decaying Bessel pulse, since fluorescence radial profile maintains Gaussian-like fast decaying (see again Fig. 5(a)) over the 10 cm long propagation.

A comparison between linearly and nonlinearly propagated pulses is shown in Fig. 6. For the Bessel pulse (Fig. 6(a)) it is clear that the combined action of Kerr focusing, dispersion and multiphoton absorption lead to a transverse compression by a factor 2 of the central spot. After a few oscillations in the first millimeters the beam width at half maximum does not change over the remaining 8 cm long propagation. A different scenario is obtained for the Gaussian profile, as can be seen in Fig. 6(b): the comparison between the linear and nonlinear propagation of the Gaussian beam shows that the pulse forms a filament in the nonlinear regime. Self focusing shrinks the FWHM from 20 to 6.5 μm but the pulse continues its propagation for only 4 equivalent Rayleigh ranges. Indeed the Rayleigh range of a Gaussian profile with 6.5 μm FWHM is 180 μm, about four time less than the propagation length of the filament generated here by competition between Kerr-nonlinearity, diffraction and nonlinear losses [12].

Finally we note that a Gaussian beam with equivalent input energy and diameter of the Bessel used in the experiment (i.e. 1mJ and 20 μm respectivelly) will induce material breakdown. Lower energies or larger radii will lead to a filamentation regime of a tightly focused pulse that is only apparently stationary over many Rayleigh ranges and that is in fact characterized by many refocusing cycles with very high local intensity peaks [13]. Such a regime is unsuitable for many practical applications.

6. Conclusions

We have explored nonlinear properties of pulsed Bessel beams by exciting 3-photon absorption in a linearly transparent material (Coumarine 120 in Methanol). We found out new feature s that make the nonlinear polarization excited by a pulsed Bessel beam much more suitable for applications than both linearly propagated pulsed Bessel beams and Gaussian beams. With

#8057 - $15.00 US
Received 8 July 2005; revised 27 July 2005; accepted 29 July 2005

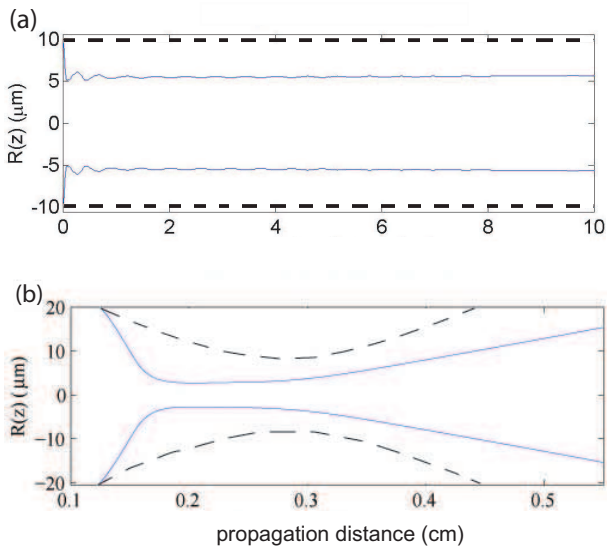

Fig. 6. (a): beam profile at half maximum of the same Bessel pulse as in Fig. 4 launched in the same Coumarine methanol solution (solid line). Dashed line corresponds to the linear propagation of the same pulse. (b): beam profile at half maximum of the same Gaussian as in Fig. 4 Gaussian beam launched in the Coumarine methanol solution (solid line), compared to its linear propagation (dashed line).

the pulsed Bessel beam we recorded an excellent improvement in contrast: while linear pulsed Bessel beams have a slowly decaying intensity profile, the nonlinear excitations triggered by the nonlinear propagation of the Bessel beam maintains a high contrast along the long focal depth of the nondiffracting central Bessel spot. In contrast with both the linear and the nonlinear propagation of pulsed Gaussian beams, arbitrary long focal depth maintaining the same desired resolution and contrast could be achieved with the pulsed Bessel beam.

These experimental evidences can lead to new applications in various fields. In multiphoton microscopy the use of conical pulses can give the possibility of reaching simultaneous great focal depth and contrast, while in photolithography [14], micromachining [15] and channel wave guide writing with longitudinal illumination one can expect to have both high contrast and resolution while keeping arbitrary long focal depth.

#8057 - $15.00 US
Received 8 July 2005; revised 27 July 2005; accepted 29 July 2005